Tunable multichannel filter in photonic crystal heterostructure containing permeability-negative materials

Xiaoyong Hu [*], Zheng Liu, Qihuang Gong [*]

State Key Laboratory for Mesoscopic Physics, Department of Physics, Peking University, Beijing 100871, PR China

Abstract

A tunable multichannel filter is demonstrated theoretically based on a one-dimensional photonic crystal heterostructure containing permeability-negative material. The filtering properties of the photonic crystal filter, including the channel number and frequency, can be tuned by adjusting the structure parameters or by a pump laser. The angular response of the photonic crystal filter and the influences of the losses on the filtering properties are also analyzed.
© 2007 Elsevier B.V. All rights reserved.

Recently, tunable photonic crystal filters have attracted great attention due to their important applications in the fields of optical communication and optical interconnection. Many schemes have been proposed to demonstrate tunable photonic crystal filters by using different materials, such as semiconductors [1–4] and ferroelectric materials [5,6]. There are large limitations for photonic crystals made from conventional dielectric materials with both positive permittivity and permeability. For example, it is difficult to achieve a high refractive index contrast needed by a wide photonic gap and strong photon confinement [7]. Photonic crystals composed of single-negative materials, i.e., materials with negative permittivity or negative permeability, can possess zero-φ_{eff} (zero effective phase) photonic gap [8]. Fang et al. reported a high-Q filter based on a one-dimensional photonic crystal using single-negative permittivity materials [7]. Chen et al. proposed a two-channel filter in a one-dimensional photonic crystal with a single-negative material defect [9]. Cheng et al. studied the properties of light propagat-

ing in a planar anisotropic biaxial slab with partially negative permittivity and permeability [10]. However, to date, little attention was paid to tunable photonic crystal filters containing single-negative materials.

In this Letter we study the tunable filtering properties of a one-dimensional photonic crystal heterostructure containing permeability-negative materials. Rhodium doped barium titanate (Rh:BaTiO$_3$) was adopted as the nonlinear optical material. As a kind of nonlinear tetragonal perovskite ferroelectric material, Rh:BaTiO$_3$ has nonlinear response time of picosecond order and very large third order nonlinear susceptibility, -5.71×10^{-7} esu [11]. The optical nonlinearity originates from the delocalization of the titanium ions in the center of TiO$_6$ octahedrons [12]. According to nonlinear optical Kerr effect, the refractive index of Rh:BaTiO$_3$ decreases under the excitation of a pump laser, so that the position and width of photonic bandgap are changed [13]. Accordingly, the optical channels shift. The dynamical tunability of the photonic crystal filter was studied in detail.

A one-dimensional photonic crystal heterostructure, also regarded as a quasiperiodic photonic structure [14], was used to construct the optical filter, as shown in Fig. 1. The structure of the optical filter is $(AB)^m(BA)^m$, where A and B represent

---

[*] Corresponding authors.
   E-mail addresses: xiaoyonghu@pku.edu.cn (X. Hu), qhgong@pku.edu.cn (Q. Gong).

permeability-negative material and Rh:BaTiO$_3$, respectively. m is the number of the repeating unit. The permittivity ε_a and the permeability μ_a of A could be written as [15]

$$\varepsilon_a = 2.3, \tag{1}$$

$$\mu_a = 1 - \frac{\omega_{mp}^2}{\omega^2 - i\omega v}, \tag{2}$$

where ω_{mp} is the plasma frequency, which was set at 2100 THz in our calculations. v is the collision frequency, which is related to loss. The value of v was set at zero and loss was not taken into account. The effective permittivity and the permeability of Rh:BaTiO$_3$ were 5.29 and 1, respectively [16]. According to our calculation, the chromatic dispersion of Rh:BaTiO$_3$ could be neglected from ultraviolet to near-infrared range. The layer
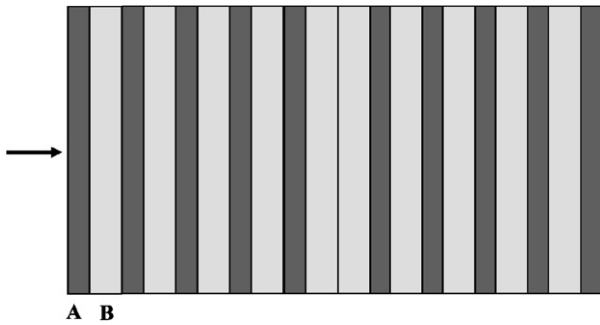
Fig. 1. Schematic of the photonic crystal heterostructure (AB)^5(BA)^5. A and B represent permeability-negative material and Rh:BaTiO$_3$, respectively. Arrow indicates the incident direction of the probe light.

thickness was 60 nm for A and 150 nm for B, respectively. The probe light, a TM polarized wave, was incident in a direction perpendicular to the A layers. The transfer matrix method was used to calculate the transmittance spectra of the photonic crystal hertostructure [17]. The transmittance spectra of the photonic crystal hertostructure (AB)^m(BA)^m with different m values were plotted in Fig. 2. Distinct photonic band gaps could be found from the transmittance spectra of the photonic crystal heterostructure. The spatially quasiperiodic distribution of the dielectric function could lead to the formation of pseudo photonic band gaps [18]. High transmittance peaks appeared in the transmittance spectra of the photonic crystal heterostructure both in the ultraviolet and near-infrared range. Negro et al. pointed out that in the frequency range outside the photonic gaps, the electromagnetic waves are critically localized with an intensity decaying less than exponentially due to the multifractal nature of the quasiperiodic photonic structure [19]. These resonant modes construct ideal optical channels. The transmittance and the quality factor of the optical channels are 100% and more than 10 000, respectively. This indicates that the optical filter possesses excellent wavelength resolution. The larger the m value is, the more the optical channel is formed. Four optical channels appeared both in the ultraviolet and near-infrared range for $m = 5$. The channel number increased to eight for $m = 10$ and twelve for $m = 15$. Fifteen optical channels could be found both in the ultraviolet and near-infrared range for $m = 20$. The photonic crystal heterostructure possesses the unique properties of structural self-similarity, which
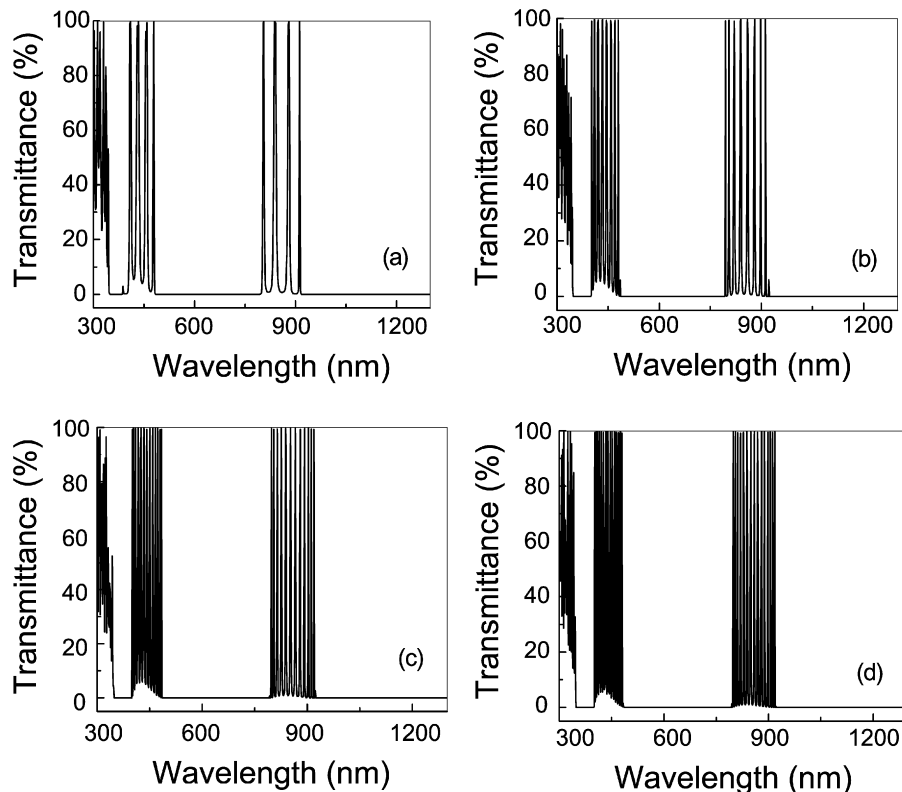
Fig. 2. Transmittance spectra of the photonic crystal heterostructure (AB)^m(BA)^m as functions of m value. (a) For $m = 5$. (b) For $m = 10$. (c) For $m = 15$. (d) For $m = 20$.
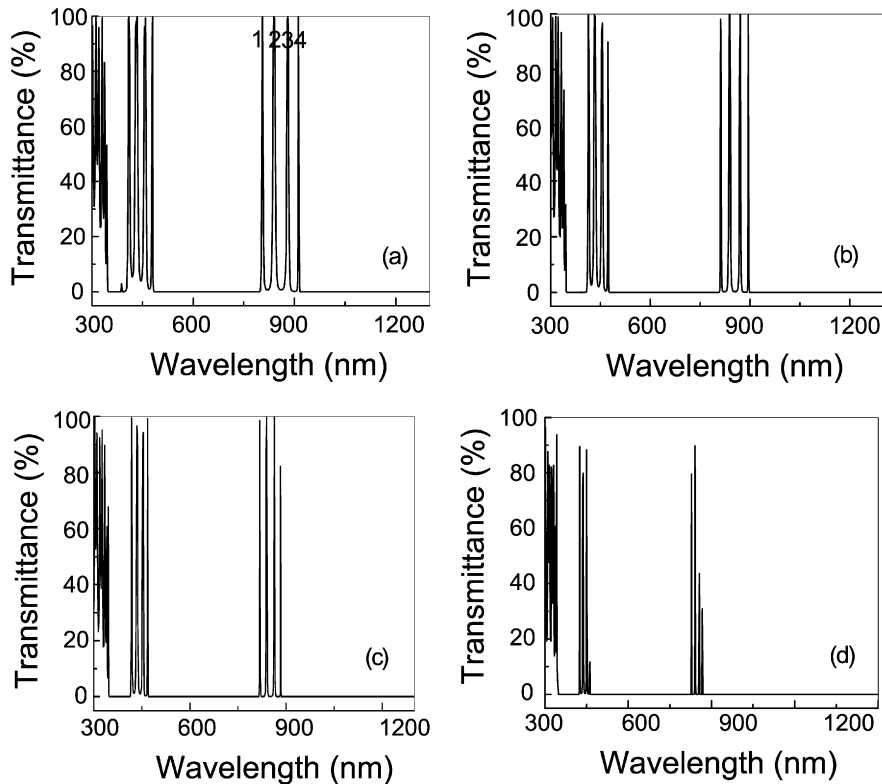
Fig. 3. Transmittance spectra of the photonic crystal heterostructure $(AB)^5(BA)^5$ as functions of the thickness of permeability-negative layers. (a) For 60 nm. The number indicates four optical channels. (b) For 70 nm. (c) For 80 nm. (d) For 100 nm.

results in the sequential splitting of the resonant modes with the increase of the layer numbers [20]. The quality factor of the optical channel increases with the increment of m value. The quality factor is more than 10 000 and 50 000 for $m = 5$ and $m = 20$, respectively. This originates from the enhancement of the photon confinement effect along with the increase of the structure unit number.

To study the tunability of the photonic crystal filter by adjusting the layer thickness, we calculated the transmittance spectra of the photonic crystal heterostructure $(AB)^5(BA)^5$ as functions of the layer thickness by the transfer matrix method. Fig. 3 depicts the transmittance spectra of the photonic crystal heterostructure $(AB)^5(BA)^5$ as functions of the thickness of permeability-negative layers. The resonant frequencies of the optical channels varied with the increase of the thickness of permeability-negative layers. For the near-infrared range, the central wavelength of channel 1 shifted in the long-wavelength direction with the increase of the thickness of permeability-negative layers. The central wavelength of channel 1 was 806 nm for a 60 nm thickness and 828 nm for a 100 nm thickness, respectively. The central wavelength of channel 2 almost sustained the original value when the layer thickness changed. The central wavelength of channel 3 and 4 shifted in the direction of short-wavelength with the increment of the thickness of permeability-negative layers. The central wavelength of channel 3 was 880 nm for a 60 nm thickness and 856 nm for a 100 nm thickness, respectively. The photonic crystal heterostructure with different layer thickness supports diverse localized resonant modes [21].

The splitting of these resonant modes leads to the changes of the central wavelengths of the optical channels. The transmittance of the optical channels decreased with the increase of the thickness of permeability-negative layers. The transmittance of four optical channels in the near-infrared range was 100% for a 60 nm thickness and less than 87% for a 100 nm thickness, respectively. This may originate from the different photon localization effect of the photonic crystal heterostructure with different thickness of permeability-negative layers. The transmittance spectra of the photonic crystal heterostructure $(AB)^5(BA)^5$ as functions of the thickness of $Rh:BaTiO_3$ layers calculated by the transfer matrix method was depicted in Fig. 4. The central wavelength of the optical channels shifted in the direction of long-wavelength with the increase of the thickness of $Rh:BaTiO_3$ layers. In the near-infrared range, the central wavelength of channel 1 was 806 nm for a 150 nm thickness and 1080 nm for a 210 nm thickness. The structure of the photonic crystal heterostructure $(AB)^5(BA)^5$ is similar to that of a Fabry–Perot (FP) dielectric microcavity [22]. The increase of the thickness of $Rh:BaTiO_3$ layers enlarges the length of the FP microcavity. This makes the resonant wavelengths of the microcavity modes shift in the direction of long-wavelength. The transmittance of the optical channels was over 90% when the thickness of $Rh:BaTiO_3$ layers changed. The similar cases occurred for the optical channels in the ultraviolet range.

To study the tunability of the photonic crystal filter, we calculated the transmittance spectra of the photonic crystal heterostructure $(AB)^5(BA)^5$ as functions of the intensity of a pump laser, as plotted in Fig. 5. Under excitation of a pump
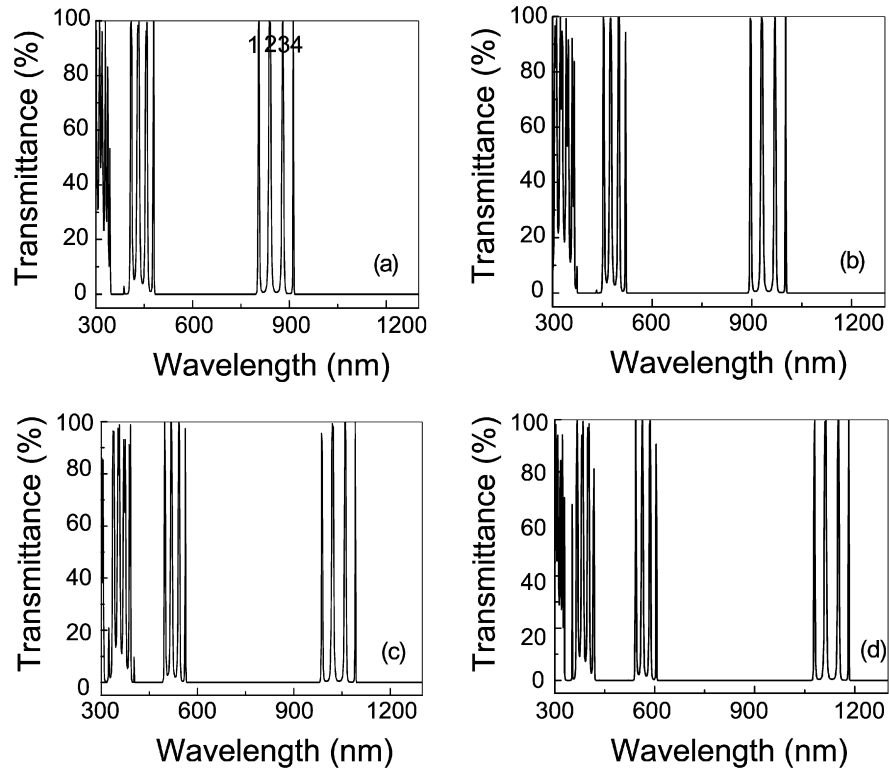
Fig. 4. Transmittance spectra of the photonic crystal heterostructure $(AB)^5(BA)^5$ with different thickness of Rh:BaTiO$_3$ layers. (a) For 150 nm. (b) For 170 nm. (c) For 190 nm. (d) For 210 nm.
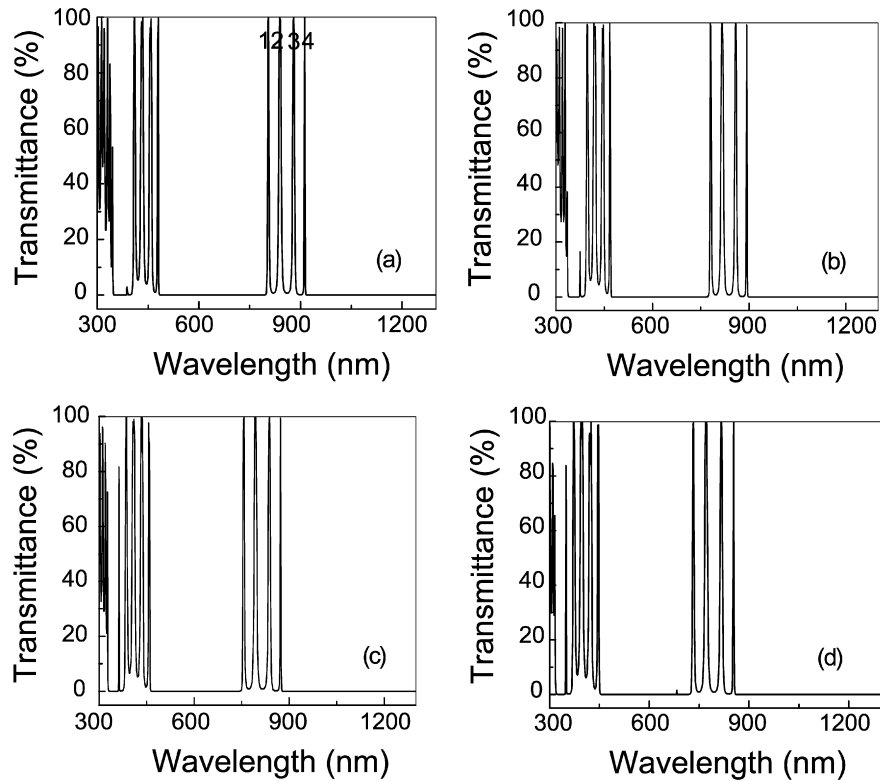
Fig. 5. Transmittance spectra of the photonic crystal heterostructure $(AB)^5(BA)^5$ as functions of the pump intensity. (a) For zero pump intensity. (b) For 25 MW/cm^2. (c) For 50 MW/cm^2. (d) For 75 MW/cm^2.
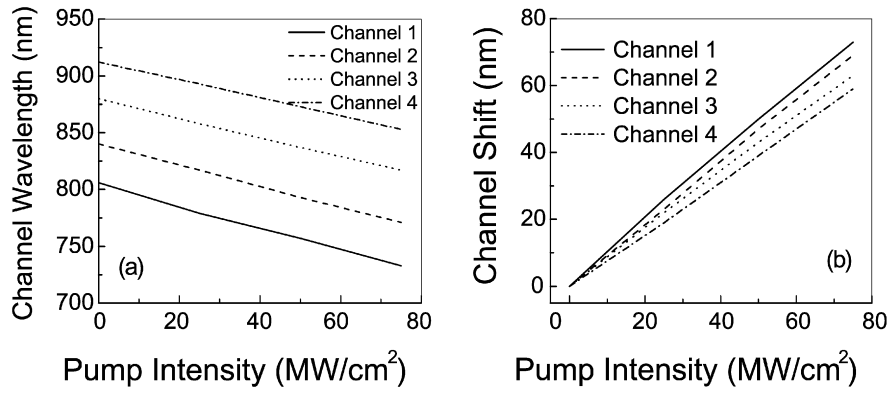
Fig. 6. Shift of the optical channels in the near-infrared range with different pump intensity. (a) For the channel central wavelength. (b) For the shift scope of the optical channels.
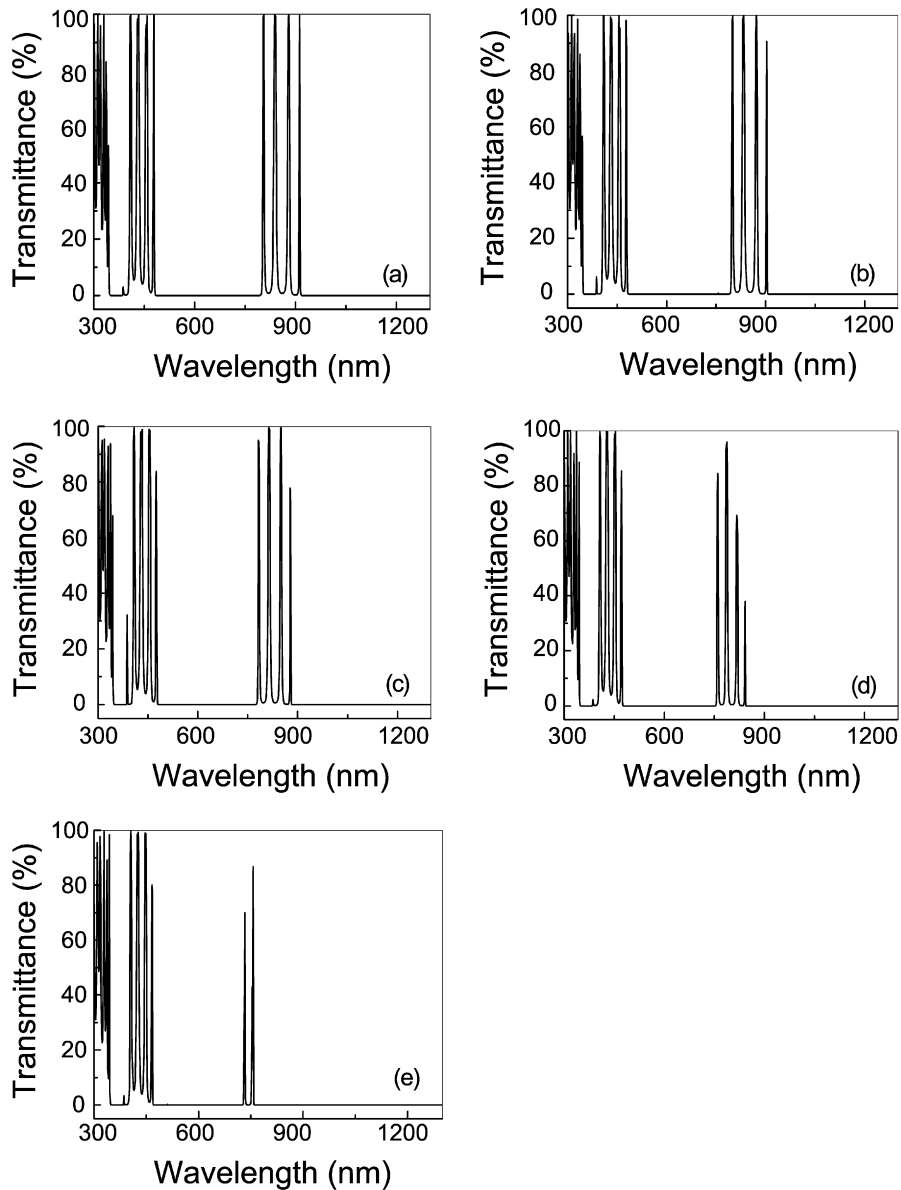
Fig. 7. Transmittance spectra of the photonic crystal heterostructure $(AB)^5(BA)^5$ as functions of the incident angle. (a) For $0°$. (b) For $5°$. (c) For $10°$. (d) For $15°$. (e) For $20°$.
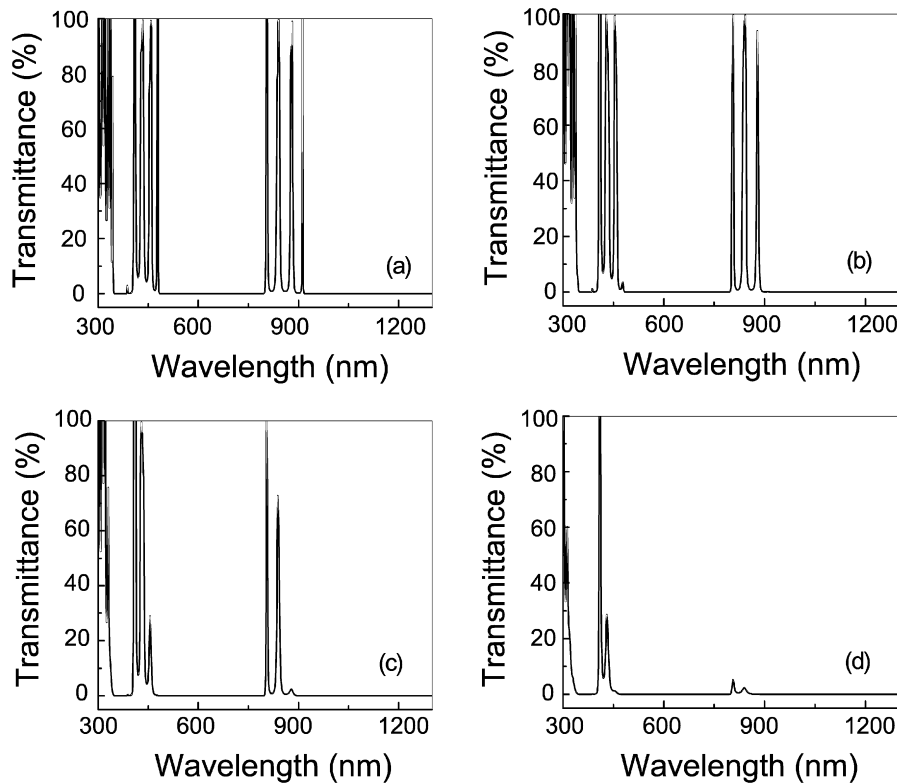
Fig. 8. Transmittance spectra of the photonic crystal heterostructure $(AB)^5(BA)^5$ with different v value. (a) For $v = 17$ THz. (b) For $v = 72$ THz. (c) For $v = 150$ THz. (d) For $v = 300$ THz.

laser, the central wavelengths of the optical channels shifted in the direction of short-wavelength. The changes of the central wavelength of the optical channels in the near-infrared range were shown in Fig. 6. The central wavelength of channel 1 was 806 nm for zero pump intensity and 733 nm for 75 MW/cm² pump intensity, respectively. The value of the third-order nonlinear susceptibility of Rh:BaTiO₃ is negative. According to the nonlinear optical Kerr effect, the refractive index of Rh:BaTiO₃ decreases under excitation of a pump laser. This results in the decrease of the effective refractive index of the photonic crystal heterostructure and the shift of the photonic bandgap in the direction of short-wavelength [23]. Accordingly, the optical channels shift in the same direction. The shift scope of the four optical channels was different with the same pump intensity. Under the excitation of a 75 MW/cm² pump laser, channel 1 shifted 73 nm, which was the maximum value among the four optical channels. The shift scope of channel 4, only 59 nm, was the minimum one among the four optical channels under excitation of the 75 MW/cm² pump laser. According to the electromagnetic variational theorem, the low frequency modes mainly concentrate their energy in the high dielectric constant regions, while the high frequency modes mainly concentrate their energy in the low dielectric constant regions [24]. As a result, the dielectric band is more sensitive to the changes of the dielectric constant of the high dielectric materials. This leads to the larger shift of the dielectric band edge. Channel 1 was situated at the dielectric band edge of the second-order photonic bandgap. The position of channel 4 was in the air band edge of the fundamental bandgap. This led to a different shift scope. The trans-

mittance and the quality factor of the optical channels changed slightly under the excitation of the pump laser. According to our calculation, the shift direction of the optical channels was independent of m value. For different m values, the optical channels shifted in the same direction of short-wavelength under excitation of a pump laser. This originates from the intensity-dependent refractive index of Rh:BaTiO₃. The shift scope of the high-frequency channels was larger than that of the low-frequency channels with the same pump intensity, which was also independent of m value. The low-frequency channels were near the air bandedge of a photonic gap. The high-frequency channels were near the dielecric bandedge of a photonic gap. The shift scope of the dielectric bandedge is larger than that of the air bandedge under excitation of the same pump intensity.

To study the angular response of the photonic crystal filter, the transmittance spectra of the photonic crystal heterostructure $(AB)^5(BA)^5$ as functions of the incident angle were calculated by the transfer matrix method and the results were depicted in Fig. 7. For the optical channels in the near-infrared range, the resonant wavelengths of optical channels do not change when the incident angle of the probe light varied from −5° to 5°. With the increase of the incident angle, the central wavelength of the optical channels shifted in the direction of the short wavelength. The reason lies in that when the incident angle changes the periodicity of the spatial distribution of the dielectric materials seen by the probe light propagating in the photonic crystal alters. When the incident angle varied from −5° to 5°, the transmittance and the quality factor of the optical channels were over 90% and about 10 000, respectively. So, less than 5° incident

angle does not destroy the filtering properties of the photonic crystal heterostructure in the near-infrared range. However, the variation of the incident angle influences the filtering properties of the photonic crystal heterostructure in the ultraviolet range very slightly. According to our calculation, with the increase of m value the resonant frequencies of the optical channels in the near-infrared range did not change when the incident angle of the probe light varied from $-5°$ to $5°$. The photonic crystal heterostructure could maintain the perfect filtering properties. With the increase of the incident angle the resonant frequencies of the optical channels in the near-infrared range shifted in the high-frequency direction, which was independent of m value. When m value changed the variation of the incident angle did not destroy the filtering properties of the photonic crystal heterostructure in the ultraviolet range. Therefore, the photonic crystal filter has a thresholdlike behavior as a function of incident angle and can sustain a certain degree of incident angle variation before remarkably weakening the filtering properties, which is independent of m value.

In order to study the influences of the losses of the permeability-negative material on the filtering properties of the photonic crystal heterostructure, we calculated the transmittance spectra of the photonic crystal heterostructure $(AB)^5(BA)^5$ as functions of v value by the transfer matrix method and the results were shown in Fig. 8. The number of optical channels decreased with the increase of v value. Four optical channels appeared for $v = 17$ THz both in the ultraviolet and near-infrared range. Only two optical channels appeared for $v = 150$ THz. The optical channel disappeared completely in the near-infrared range for $v = 300$ THz. The quality factor of the optical channels decreased with the increase of v value. The quality factor was 5000 for $v = 72$ THz and 3000 for $v = 150$ THz, respectively. The transmittance of the optical channels decreased with the increase of v value. However, for $v = 17$ THz, the transmittance of the optical channels was about 100% and the quality factor was over 7000. The photonic crystal heterostructure can maintain excellent filtering properties when v is less than 17 THz.

In conclusion, we have theoretically demonstrated a tunable multichannel photonic crystal filter containing permeability-negative materials. The filtering properties, including the channel number and frequency, could be tuned by adjusting the structure structures or by a pump laser. These results may be useful for the study of integrated photonic devices based on single-negative materials.

References

[1] D.K. Jacob, S.C. Dunn, M.G. Moharam, Appl. Opt. 41 (2002) 1241.
[2] M. Qiu, B. Jaskorzynska, Appl. Phys. Lett. 83 (2003) 1074.
[3] K. Hennessy, A. Badolato, A. Tamboli, P.M. Petroff, E. Hu, M. Atature, J. Dreiser, A. Imamoglu, Appl. Phys. Lett. 87 (2005) 021108.
[4] Y. Pennec, B.D. Rouhani, A. Akjouj, J.O. Vasseur, L. Dobrzynski, J.P. Vilcot, M. Beaugeois, M. Bouazaoui, R. Fikri, J.P. Vigneron, Appl. Phys. Lett. 89 (2006) 101113.
[5] M.F. Yanik, S.H. Fan, M. Soljacic, Appl. Phys. Lett. 83 (2003) 2739.
[6] B.K. Min, J.E. Kim, H.Y. Park, Opt. Commun. 237 (2004) 59.
[7] Y.T. Fang, J. Zhou, E.Y.B. Pun, Appl. Phys. B 86 (2007) 587.
[8] S.M. Wang, C.J. Tang, T. Pan, L. Gao, Phys. Lett. A 348 (2006) 424.
[9] Y.H. Chen, J.W. Dong, H.Z. Wang, Appl. Phys. Lett. 89 (2006) 141101.
[10] Q. Cheng, T.J. Cui, Appl. Phys. Lett. 87 (2005) 174102.
[11] W.S. Shi, Z.H. Chen, N.N. Liu, H.B. Lu, Y.L. Zhou, D.F. Cui, G.Z. Yang, Appl. Phys. Lett. 75 (1999) 1547.
[12] Y. Guang, H.H. Wang, G.T. Tan, A.Q. Jiang, Y.L. Zhou, G.Z. Yang, Z.H. Chen, Chin. Phys. Lett. 18 (2001) 1598.
[13] P.M. Johnson, A.F. Koenderink, W.L. Vos, Phys. Rev. B 66 (2002) 081102(R).
[14] H.Y. Zhang, Y.P. Zhang, T.Y. Shang, Y. Zheng, G.J. Ren, P. Wang, J.Q. Yao, Eur. Phys. J. B 52 (2006) 37.
[15] X.S. Rao, C.K. Ong, Phys. Rev. B 68 (2003) 113103.
[16] X.Y. Hu, Q.H. Gong, S. Feng, B.Y. Cheng, D.Z. Zhang, Opt. Commun. 253 (2005) 138.
[17] L.G. Wang, H. Chen, S.Y. Zhu, Phys. Rev. B 70 (2004) 245102.
[18] Z.S. Wang, L. Wang, Y.G. Wu, L.Y. Chen, X.S. Chen, W. Lu, Appl. Phys. Lett. 84 (2004) 1629.
[19] L.D. Negro, C.J. Oton, Z. Gaburro, L. Pavesi, P. Johnson, A. Lagendijk, R. Righini, M. Colocci, D.S. Wiersma, Phys. Rev. B 90 (2003) 055501.
[20] M. Maksimovic, Z. Jaksic, J. Opt. A: Pure Appl. Opt. 8 (2006) 355.
[21] R.W. Peng, M. Wang, A. Hu, S.S. Jiang, G.J. Jin, D. Feng, Phys. Rev. B 57 (1998) 1544.
[22] A.V. Lavrinenko, S.V. Zhukovsky, K.S. Sandomirski, S.V. Gaponenko, Phys. Rev. E 65 (2002) 036621.
[23] X.Y. Hu, Y.Q. Wang, Y.H. Liu, B.Y. Cheng, D.Z. Zhang, Opt. Commun. 237 (2004) 371.
[24] J.D. Joannopoulos, R.D. Meade, J.N. Winn, Photonic Crystals: Molding the Flow of Light, Princeton Univ. Press, Princeton, 1995.